Published in final edited form as:
Biochemistry. 2011 April 19; 50(15): 3149–3160. doi:10.1021/bi101796m.

Functional and structural roles of residues in the third extra-membrane segment (EM3) of adrenal cytochrome b_{561}[†]

Wen Liu[1,#], **Giordano F.Z. da Silva**[1,2,#], **Gang Wu**[1], **Graham Palmer**[2], **Ah-Lim Tsai**[1], and **Richard J. Kulmacz**[1,*]

[1] Department of Internal Medicine, University of Texas Health Science Center, Houston, TX 77030

[2] Department of Biochemistry & Cell Biology, Rice University, Houston, TX 77251

Abstract

Several residues in the third extramembrane segment (EM3) of adrenal cytochrome b_{561} have been proposed to be involved in this cytochrome's interaction with ascorbate, but there has been no systematic evaluation of residues in the segment. We used alanine-scanning mutagenesis to assess the functional and structural roles of the EM3 residues and several adjacent residues (residues 70–85) in the bovine cytochrome. Each alanine mutant was expressed in a bacterial system, detergent solubilized, and affinity purified. The recombinant proteins contained ~two hemes/monomer and, except for R74A, retained basic functionality (≥ 94% reduced by 20 mM ascorbate). Equilibrium spectrophotometric titrations with ascorbate were used to analyze the alpha band lineshape and amplitude during reduction of the high- and low-potential heme centers (b_H and b_L, respectively), and the midpoint ascorbate concentrations for the b_H and b_L transitions (C_H and C_L, respectively). Y73A and K85A markedly narrowed the b_H alpha band peak; other mutants had lesser or no effects on b_H or b_L spectra. Relative changes in C_H for the mutants were larger than changes in C_L, with increases of 1.5- to 2.9-fold in C_H for L70A, L71A, Y73A, R74A, N78A and K85A. The amounts of functional b_H and b_L centers in additional Arg74 mutants, assessed by ascorbate titration and EPR spectroscopy, declined in concert in the order: wildtype > R74K > R74Q > R74T, R74Y > R74E. The results of this first comprehensive experimental test of the proposed roles of EM3 residues have identified residues with direct or indirect impact on ascorbate interactions, on the environment of the b_H heme center, and on formation of the native b_H/b_L unit. Surprisingly, no individual EM3 residue was by itself indispensable for the interaction with ascorbate, and the role of the segment appears to be more subtle than previously thought. The present results also support our topological model of the adrenal cytochrome, which positions b_H near the cytoplasmic side of the membrane.

[†]Support: National Institutes of Health grant GM 080575

[*]Address correspondence to Dr. Kulmacz at: Department of Internal Medicine, University of Texas Health Science Center, 6431 Fannin Street, MSB 5.016, Houston, TX 77030, Phone: 713 500 6772, Fax: 713 500 6812, richard.j.kulmacz@uth.tmc.edu.
[#]These two authors contributed equally.

Supporting Information Available

Supplementary material from this study includes sequence information for the mutagenic primers, absorbance spectra observed during ascorbate titrations of additional cyt b_{561} mutants, difference spectra of b_H and b_L heme centers for additional cyt b_{561} mutants, deconvolution of b_H heme spectral components, EPR signal amplitudes in Arg74 mutants, and tabulated data for the various mutants studied. This material is available free of charge via the Internet at http://pubs.acs.org.

Adrenal cytochrome b_{561} (cyt b_{561})[1] is an integral membrane protein that shuttles reducing equivalents from cytoplasmic ascorbate across the membrane and into the matrix of chromaffin granules to support catecholamine biosynthesis (1). Cyt b_{561} contains two b-type heme centers, with redox potentials of ~170 mV (high-potential, b_H) and ~60 mV (low-potential, b_L) (2, 3). Cyt b_{561} is the prototype of a family of diheme cytochromes that are widely distributed among animal and plant species (4). As it is by far the best-studied member of the family, cyt b_{561} has many advantages as an experimental model for structural and mechanistic studies. The currently accepted membrane topology for the cyt b_{561} polypeptide, based originally on sequence analysis (5), has six alpha-helical transmembrane segments, four extramembrane segments exposed towards the cytoplasm (EM1, EM3, EM5, and EM7), and three extramembrane segments exposed to the lumenal compartment (EM2, EM4, and EM6) (Fig. 1). The positions of the b_H and b_L centers in the chromaffin granule membrane have been controversial, with one model assigning b_H to the His88/His161 heme (as depicted in Fig. 1) (6, 7), and an earlier model assigning b_H to the His54/His122 heme (8, 9). A key issue from a mechanistic perspective is whether it is b_H or b_L that is exposed to the cytoplasm and its pool of ascorbate.

Previous efforts to map the residues important to interaction with ascorbate in the cytoplasm have focused almost entirely on residues in EM3. Several residues in and adjacent to EM3 in bovine cyt b_{561} are strongly conserved among close homologs from many organisms (4). Residues 69–77 (ALLVYRVFR), which comprise the N-terminal part of EM3 and flanking residues in TM2, were proposed to be part of an ascorbate interaction site on the cytosolic side of the membrane, based on both sequence conservation and anticipated electrostatic interactions between strongly anionic ascorbate and the positively charged residues in the segment (10). The C-terminal part of EM3 has three additional positively charged residues at positions 81, 82, and 85 (Fig. 1). Some of the conserved residues in EM3 have turned up in chemical modification studies and others have been targeted by site-directed mutagenesis (1, 11–14). However, there has not been a systematic evaluation of the roles of individual EM3 residues in the reduction by ascorbate of the b_H and b_L heme centers. The two heme centers and the four helices carrying them (TM2, TM3, TM4, and TM5 in Fig. 1) have been proposed to be part of a larger structural unit, termed the kernel, whose integrity is required for proper membrane insertion and folding of the 6-helix cytochrome (6, 7). The kernel in adrenal cyt b_{561} can be disrupted as a unit by even relatively conservative mutations in any one of the four histidines furnishing an axial ligand to one of the hemes (6, 7). EM3 terminates with Lys85, which is three residues from His88, the axial heme ligand in TM3 (Fig. 1), raising the possibility that one or more residues in EM3 also are part of the structural kernel.

Alanine scanning mutagenesis is a well-established approach to systematic evaluation of the structural and functional roles of individual residues in a targeted polypeptide (15). As the first comprehensive, experimental test of the proposed roles of conserved EM3 residues in reduction of the cytochrome by ascorbate and of the disposition of EM3 with respect to the two heme centers, we applied the alanine scanning approach to residues 70–85 of bovine adrenal cyt b_{561} (except Ala80). Given the proposed importance of EM3 residues to the interaction with ascorbate, it was anticipated that one or more of these alanine mutants would lack the ability to react with ascorbate yet retain native structure at the heme centers. The recombinant proteins were expressed in an *E. coli* system, solubilized with detergent, purified by affinity chromatography, and characterized in spectrophotometric ascorbate titrations to evaluate the effect(s) of each mutation on the structure and function of the

[1]The abbreviations used are: cyt b_{561}, adrenal cytochrome b_{561}; EM, extra-membrane segment; TM, transmembrane segment; b_H and b_L, high- and low-potential heme centers, respectively; C_H and C_L, midpoint ascorbate concentrations for the b_H and b_L ferric-ferrous transitions, respectively; EPR, electron paramagnetic resonance spectroscopy;

individual b_H and b_L heme centers. Alanine substitution at Arg74 produced major structural disruptions, and a series of additional Arg74 mutations were characterized by ascorbate titration and EPR spectroscopy to evaluate the role of sidechain charge and polarity at this position on formation of the native b_H/b_L unit.

EXPERIMENTAL PROCEDURES

Materials

Hemin, ascorbic acid, sodium ascorbate, δ-aminolevulinic acid, isopropyl-1-thio-β-D-galactopyranoside, ampicillin, chloramphenicol, and egg lysozyme were from Sigma (St. Louis, MO). n-Dodecyl-β-D-maltoside was from Anatrace (Maumee, OH). Restriction enzymes and other DNA modifying enzymes were purchased from New England Bio-Labs (Beverly, MA). Oligonucleotides were obtained from Integrated DNA Technologies (Coralville, IA). Plasmid vector pET43.1a, Benzonase nuclease, and Protease Inhibitor Cocktail Set III (without EDTA) were purchased from Novagen (Madison, WI). *E. coli* strains BL21Star(DE3) was from Invitrogen (Carlsbad, CA). The chaperone plasmid, pT-groE, was generously provided by Dr. Lee-Ho Wang (University of Texas Health Science Center at Houston). TALON metal affinity resin was purchased from BD Biosciences Clontech (Palo Alto, CA). DNA sequencing was performed at the Microbiology and Molecular Genetics Core Facility, University of Texas Health Science Center at Houston (Houston, TX).

Expression and purification of His-tagged recombinant cyt b_{561} proteins

Construction of the pET43.1a plasmid containing sequence coding for the full-length bovine adrenal cyt b_{561}, designated pET43.1a-b_{561}C6H, is described elsewhere (16). Point mutations were introduced using the QuikChange site-directed mutagenesis kit (Stratagene, La Jolla, CA) and the pET43.1a-b_{561}C6H expression plasmid as the template. Each set of mutagenic primer (sense) (Supplementary Material, Table S1) and its complementary (antisense) strand was used in a PfuUltra polymerase-initiated reaction. The original, methylated DNA strand was digested with DpnI, and the remaining DNA was transformed into *E. coli* XL1-Blue competent cells. Each mutant construct was validated by restriction digests and DNA sequencing. The wild type cyt b_{561} and EM3 mutants were expressed in the BL21Star(DE3)/pT-groE *E. coli* strain and purified according to published procedures (16).

Assay of protein, cyt b_{561}, and heme content

Total protein was assayed with a modified Lowry method using bovine serum albumin as the standard (17). Recombinant cyt b_{561} content was calculated using a reduced (dithionite-treated) minus oxidized (ferricyanide-treated) difference extinction coefficient (561–575 nm) of 34 mM^{-1} cm^{-1} (18, 19). Heme content was determined by the pyridine hemochrome method (19) using an extinction coefficient difference (556–538 nm) of 24.5 mM^{-1} cm^{-1} (20). The homogeneity of purified proteins was determined by densitometry (ImageJ software from NIH) of Coomassie blue-stained bands after separation of proteins (~1 μg/lane) by polyacrylamide gel electrophoresis under denaturing conditions (21). The heme stoichiometry of each purified recombinant protein was calculated from its heme concentration (determined by pyridine hemochrome assay) and its monomer concentration (determined by total protein assay and electrophoretic analysis).

Ascorbate titrations of wild type and mutant cyt b_{561}

Ascorbate titrations were performed as previously published with minor changes (7). Pre-oxidized cyt b_{561} samples (5–11 μM) in 100 mM potassium phosphate buffer (pH 7.2)

containing 18% glycerol and 0.08% (w/v) n-dodecyl-β-D-maltoside were placed in a 1-cm quartz cuvette. The titrations used 17–21 levels of ascorbate, typically between 0.13 μM and 20 mM, but extending to 90 mM for ascorbate-resistant samples. The system was allowed to restabilize completely (5 min) after each addition of ascorbate before the spectrum was collected. Spectra were recorded in a Shimadzu Model UV-2101PC or UV-2401PC spectrophotometer with a scan rate of 20 nm/min, with 20 data points/nm and a spectral bandwidth of 0.5 or 1 nm. All ascorbate stock solutions were at pH 7.2, freshly made from mixtures of ascorbic acid and sodium ascorbate, and were kept on ice and protected from light. The increases in A_{561} were corrected for dilution. In some cases, oxygen was purged with several cycles of vacuum and argon replacement and the titration was performed under anaerobic conditions; removing oxygen did not change the results significantly. For wildtype cyt b_{561} and the mutants found to be at least 93% reduced by 20 mM ascorbate the increases in A_{561} during titration were fitted by nonlinear regression to a two-phase, four-parameter equation:

$$\Delta A_{561}=\Delta A(b_H)/(1+C_H/[\mathrm{Asc}])+\Delta A(b_L)/(1+C_L/[\mathrm{Asc}]) \quad \text{(Eq. 1)}$$

Here, [Asc] is the ascorbate concentration, $\Delta A(b_H)$ and $\Delta A(b_L)$ are overall absorbance changes for the high- and low-potential heme transitions, respectively, and C_H and C_L are midpoint ascorbate concentrations for the high- and low-potential heme center transitions, respectively.

Some mutants were found to require ascorbate levels above 20 mM, or even dithionite (~1 mM), for complete reduction, indicating that a portion of the recombinant cytochrome had one or more non-native forms of heme center with unusually low redox potential. For these mutants, the increases in A_{561} during the titration were fitted to a three-phase, six-parameter equation:

$$\Delta A_{561}=\Delta A(b_H)/(1+C_H/[\mathrm{Asc}])+\Delta A(b_L)/(1+C_L/[\mathrm{Asc}])+\Delta A(b_{VL})/(1+C_{VL}/[\mathrm{Asc}]) \quad \text{(Eq. 2)}$$

The additional parameters, $\Delta A(b_{VL})$ and C_{VL}, are the overall absorbance change and midpoint ascorbate concentration, respectively, for the very low-potential heme center. Note that any heme that is unreactive with ascorbate and reduced only by dithionite is not included in this fitting.

EPR spectroscopy

Samples of wildtype and mutant cytochromes were concentrated and oxidized before recording EPR spectra at 4 or 8 K as described previously (7). The spectrometer settings were: microwave frequency, 9.58 GHz; modulation frequency, 100 kHz; modulation amplitude, 10.9 G; and power, 4 mW. EPR spectra of purified N78K and H110Q mutants (7) recorded at both 4 and 8 K were used to calculate the temperature dependence of individual signals at g= 2.95, 3.1 and 3.7.

RESULTS

Expression and purification

The level of recombinant protein expressed in the bacterial system varied considerably among the EM3 alanine mutants (Supplementary Material, Table S2). Most mutants were expressed at levels comparable to the wildtype protein. R82A and K85A were expressed at somewhat higher levels, R74A at somewhat lower levels, whereas E79A and K81A expression levels were poor. Nevertheless, the bulk of each of the recombinant proteins was

solubilized with nonionic detergent, an indication of proper folding and membrane insertion (7), and each could be purified in sufficient yield for characterization. The electrophoretic homogeneity of the purified proteins was ~85% except for the few poorly expressing mutants, where the homogeneity was ~70%.

Heme stoichiometry and reactivity with ascorbate

As expected from previous results (7, 16) the heme content of wildtype cyt b_{561} was almost exactly two per monomer (Supplementary Material, Table S2), showing that most modifications of EM3 sidechains did not prevent incorporation of a full heme complement into the protein. The basic functionality of each recombinant protein was assessed by comparison of the intensity of alpha band absorbance from cytochrome reduction upon addition of 20 mM ascorbate to that upon complete reduction by dithionite (Supplementary Material, Table S2; full spectra of wildtype cytochrome and selected mutants are in Fig. S5). Wildtype cyt b_{561} was 97% reduced, and the EM3 alanine mutants were also quantitatively reduced (i.e., 94–98%), except for R74A, which only was 45% reduced. These results indicate that only the R74A mutation resulted in formation of a considerable fraction of cytochrome that did not react with ascorbate. Ascorbate reducibility values of 75–85% were reported in other studies of native and recombinant cyt b561 (e.g., refs. 7–9). These instances of lower reducibility probably reflect the use of lower concentrations of ascorbate, less purified cytochrome preparations, or differences in buffer composition. Characterization of additional Arg74 mutations is described below.

Reaction of high- and low-potential heme centers with ascorbate

Analyses of alpha band absorbance changes during titration of cyt b_{561} family members with ascorbate have proven quite informative for assessing the impact of mutations on the individual heme centers (6, 7, 22). Accordingly, ascorbate titrations were performed on wildtype cyt b_{561} and each of the purified EM3 alanine mutants. Examples of the resulting sets of absorbance spectra are shown for the wildtype cytochrome and the Y73A and R74A mutants in Fig. 2 (spectral data for the other mutants are included in Supplementary Material, Fig. S1). In each case, the alpha band absorbance increased with increases in added ascorbate. For the wildtype cytochrome and most of the EM3 alanine mutants, a shoulder near 554 nm was apparent in addition to the main peak near 561 nm (Fig. 2), as observed previously (7). The shoulder near 554 nm was not apparent in the Y73A titration (Fig. 2), and the overall absorbance increase during the titration was markedly smaller for the R74A mutant (Fig. 2), as expected from the lower reactivity with ascorbate in this mutant (Supplementary Material, Table S2). The progression of each titration was monitored by plotting the ΔA at 560–561 nm as a function of the added ascorbate concentration. Examples are shown in the upper panel of Fig. 3 for the wildtype and the Y73A and R74A mutants. The data for the wildtype cytochrome and all of the alanine mutants except R74A fit well to Eq. 1, which describes two independent and saturable phases of absorbance transition. The first transition, that of a high-potential heme center (b_H), had a midpoint ascorbate concentration (C_H) in the range of 2–15 μM (Fig. 3, top and bottom). The second transition, that of a low-potential heme center (b_L), had a midpoint ascorbate concentration (C_L) between 170 and 810 μM. The proportions of ΔA_{561} in the first and second transitions varied considerably, as exemplified by the results for wildtype (0.60:0.40) and Y73A (0.40:0.60) (Fig. 3, upper panel). The titration data for R74A were found to fit rather poorly to Eq. 1 for the two-transition model (Supplementary Material, Fig. S2). This appeared to be due to the considerable portion of recombinant hemoprotein that was reduced only at very high ascorbate levels. Accordingly, the equation for a three-transition model (Eq. 2) was tried instead. Eq. 2 was found to fit the R74A data quite well (Fig. 3, upper panel), and the fitted amplitude parameters indicated that ~30% of the absorbance change was associated with b_H (C_H ~20 μM), ~45% with b_L (C_L ~300 μM) and ~25% with very low-potential

heme or "b_{VL}" (C_{VL} ~8 mM). The purified R74A protein thus contained decreased but distinct portions of cytochrome with midpoint ascorbate concentrations comparable to those of the native b_H and b_L heme centers, in addition to a non-native population that was reduced only at high ascorbate levels (b_{VL}) and yet another population that was refractory to ascorbate and required dithionite for reduction (termed b_X; not shown in Fig. 3). It is important to note that no more than two hemes were present per monomer in any of the purified recombinant proteins (Supplementary Material, Table S2). Thus, b_{VL} and b_X do not represent a third or fourth heme center but rather altered forms of b_H and/or b_L produced by structural or folding perturbations in the recombinant proteins. There is at least one well-characterized precedent for expression of multiple forms of a recombinant cytochrome other than cyt b_{561} in heterologous systems (23).

Absorbance spectra of the b_H and b_L heme centers

Before analyzing the quantitative differences in C_H and C_L values observed in the ascorbate titrations of the mutants (such as those shown in Fig. 3, top panel) it was important to determine whether individual mutations affected the structure of either heme center. Due to the ~110 mV separation of midpoint potential between the two heme centers, alpha band difference spectra from early (ascorbate < C_H) and late (ascorbate > C_L) phases in an ascorbate titration provide a way of separately analyzing the spectra of the b_H and b_L centers, respectively (7). The strategy is outlined in the lower panel of Fig 3, with the difference spectra for b_H obtained by subtracting the spectrum at point A from that at point B reflecting contributions almost exclusively from b_H and the spectrum at point C from that at point D reflecting contributions almost exclusively from b_L. The resulting difference spectra for the b_H and b_L centers of the Y73A, R74A, R77A and K85A mutants are shown in Fig. 4, superimposed on the corresponding wildtype spectra. It is important to note that these difference spectra arise specifically from recombinant protein containing b_H and b_L, thus providing a way to selectively characterize these species even for a mutant such as R74A where most of the recombinant protein produced has non-native cytochrome that is resistant to, or unreactive with, ascorbate.

The b_H spectrum of the Y73A mutant lacked the shoulder at ~554 nm seen with the wildtype cytochrome, making the mutant b_H spectrum narrower and more symmetric. The b_H spectrum of the K85A mutant was also narrowed, though to a slightly lesser degree than with Y73A (Fig. 4A). In contrast, the b_H spectra of R74A and R77A had essentially the same peak width as the wildtype, though the shoulder on the shorter wavelength side was less pronounced in R74A. None of the other alanine mutants in EM3 produced significant changes in the b_H spectrum (Supplementary Material Fig. S3). The b_L spectra for the four mutants shown in Fig. 4B had only subtle differences from the corresponding wildtype spectrum. The b_L peak was shifted to slightly shorter wavelength in Y73A, and was slightly broadened in R74A, but the b_L spectra for R77A and K85A were almost superimposable on the wildtype spectrum. The b_L spectra for the other EM3 alanine mutants were also little different from the wildtype spectrum, except for L70A and T83A, which were slightly blue-shifted (Supplementary Material, Fig. S3). The b_H alpha bands for wildtype cytochrome and the Y73A and K85A mutants were also analyzed by deconvolution into Gaussian components (Supplementary Materials, Fig. S6). The Y73A mutant showed a large decrease in amplitude of the component near 555 nm compared to wildtype; the amplitude of the component at 555 nm was also slightly decreased in the K85A mutant.

Effects of EM3 alanine mutations on ascorbate titration parameters

Between two and six independent ascorbate titrations were performed for each of the EM3 alanine mutants. Data from each titration were fitted to Eq. 1 (Eq. 2 for R74A) to quantify the amplitude and midpoint ascorbate concentration for the b_H, b_L and b_{VL} (if present)

transitions, as described above. To simplify evaluation of mutational effects, the two amplitudes were combined as a ratio, $\Delta A_H/\Delta A_L$. One notable overall observation from the results, shown in Fig. 5, is that each of the EM3 mutants except E79A and T84A had a statistically significant ($p < 0.05$) effect on at least one of the three ascorbate titration parameters examined. This suggests that the functional interaction of cyt b_{561} with ascorbate directly or indirectly involves many EM3 residues, not just one or two. None of the mutations in EM3 residues completely blocked reduction of either heme center, indicating that none of these residues by itself is essential to redox interaction with ascorbate. A further overall observation is that the effects on the value of C_H tended to be considerably larger than those on the value of C_L. The simplest interpretation of this outcome is that EM3 is positioned closer to b_H than to b_L. As EM3 is currently accepted as being exposed to the cytoplasm (24), it follows that the b_H heme center is oriented toward the cytoplasmic face of the chromaffin granule membrane. This gives further support to the assignment of b_H to the heme ligated by the His88/His161 ligand pair (6, 7), as depicted in Fig. 1.

To focus on EM3 residues whose sidechain structures have a larger functional impact, thresholds are drawn in Fig. 5 to indicate parameter increases by a factor of 1.5 and decreases by a factor of 1/1.5, each relative to the wildtype value. Alterations in C_L exceeded the threshold factor of 1.5 only in five mutants, with an increased C_L in Y73A and decreased C_L in V72A, F76A, R77A, R82A and T83A (Fig. 5). All of these residues are a considerable distance (~2 nm) from the b_L heme in the model, suggesting that the effects of these mutations on C_L are indirect and reflect longer-range structural perturbations.

Only Y73A, R74A and K85A showed alterations in the $\Delta A_H/\Delta A_L$ ratio beyond the threshold; all showed a decreased ratio (Fig. 5). At present, there are no crystallographic data for cyt b_{561} or for a related protein suitable for homology modeling. However, Bashtovyy et al. (25) have developed a computational model of cyt b_{561} that is useful for tentative interpretation of the present results. This model includes transmembrane helices 2–5, which carry the four histidines that have been shown to provide axial ligands for the two hemes. The main constraints in the modeling were the His-heme-His crosslinking between helices 2 and 4 and helices 3 and 5, and the disposition of hydrophobic sidechains in the transmembrane segments towards the outside of the four-helix bundle (25). The predicted proximity of Tyr73 and Lys85 to one heme in this computational model (Fig. 6) would be consistent with the observed change in absorbance ratio for the Y73A and K85A mutants. On the other hand, the Arg74 sidechain is predicted to be oriented away from the heme (Fig. 6A). If this aspect of the model is correct, it appears inconsistent with invoking a direct effect to explain the altered absorbance ratio in R74A.

The alanine mutants of several charged and polar residues in EM3 exhibited little or no difference from the wildtype cytochrome in the ascorbate titration parameters (Fig. 5). The predicted dispositions of the sidechains of these residues are depicted in Fig. 6B. Four of these sidechains (Lys81, Arg82, Thr83 and Thr84) are clustered near the C-terminal end of EM3 and radiate outward from the four-helix bundle. This suggests that this part of EM3 does not have important interactions with ascorbate or with other parts of the protein. The sidechain of Glu79 is predicted to be some distance from the b_H heme, projecting away (Fig. 6B); this orientation seems quite consistent with the lack of effects seen with E79A (Fig. 5).

Mutational analysis of Arg74

As noted above, R74A was the only EM3 alanine mutation that markedly impaired reduction of cyt b_{561} by ascorbate (Supplementary Material, Table S2). The role of Arg74 was further evaluated with additional mutations to vary the sidechain charge and polarity at this position (R74K, R74Q, R74T, R74Y, and R74E). Each of these recombinant proteins

(his-tagged at the C-terminus) was expressed in the bacterial system, solubilized with detergent, and purified by affinity chromatography, as described for the alanine mutants.

The basic characteristics of the Arg74 mutants are presented in Table S3 (Supplementary Material). Each was expressed in at least moderate yield, except for R74E. The heme stoichiometry ranged from 1.9 to 1.7, indicating that the disruptive effects on heme incorporation of the Arg74 mutants varied from very mild (e.g., R74K) to quite significant (e.g., R74E). The general functionality, assessed as the fraction of cytochrome reducible by 20 mM ascorbate, was 91% for R74K, only slightly lower than the wildtype value. The ascorbate reducibility decreased to 81% in R74Q and R74T and was precipitously lower in the R74A (45%), R74Y (35%), and R74E (9%) mutants. The proportion of functional cytochrome in the purified recombinant protein thus decreased progressively as the sidechain at position 74 went from positively charged to neutral polar to aromatic to negatively charged.

Ascorbate titrations were used for detailed characterization of each of the Arg74 mutants except for R74E, whose very low reducibility by ascorbate made titration impractical. Two reductive transitions were observed for R74K (b_H and b_L, as with wildtype cytochrome in Fig. 3), whereas all of the other Arg74 mutants showed three reductive transitions (b_H, b_L, and b_{VL}; as for R74A in Fig. 3). The b_H and b_L spectra obtained from titrations of the Arg74 mutants, using the difference approach outlined in the lower panel of Fig. 3, are shown in Fig. S4 (Supplementary Material). The b_H spectrum was little different from the wildtype in R74K, R74Q and R74T, but the shoulder was clearly shifted from 554 nm to longer wavelengths in the R74A and R74Y mutants. The b_L spectrum was indistinguishable from wildtype in R74K, but noticeably wider than wildtype in each of the other Arg74 mutants, with R74Y presenting the largest changes. Thus, modifications at Arg74 that removed the positive charge altered the b_L spectrum, and the b_H spectrum as well for the alanine and tyrosine substitutions. Note that the patterns of spectral perturbation in R74Q and R74T represent unusual instances where mutation of an EM3 residue affect a property of the b_L heme center more than that of the b_H heme center.

The values of C_H, C_L and C_{VL} calculated from the ascorbate titrations of the Arg74 mutations are shown in Fig. 7A. Each of the mutants except R74T had a C_H value significantly higher than that for wildtype cytochrome, and there was a trend to increasing C_H value in the order: WT < R74T < R74K < R74Q < R74A < R74Y. In contrast, the values of C_L for the mutants were similar to the wildtype value (Fig. 7A). R74Y had a higher C_{VL} value than the other three Arg74 mutants exhibiting a significant b_{VL} transition, but the uncertainties in estimating C_{VL} were large and there was no obvious trend to the data.

The ascorbate titrations of the Arg74 mutants were also analyzed to quantitate the amplitudes of ΔA_{560} associated with the b_H, b_L, and b_{VL} transitions (Fig. 7B). The ΔA_{560} amplitudes were normalized to the heme concentration in order to estimate the contribution of individual ascorbate-reducible heme centers in each purified hemoprotein sample. In the wildtype cyt b_{561}, the b_H and b_L transitions produced ΔA_{560}/heme values of ~16 and ~11 $(mM)^{-1}$, respectively, for an overall ascorbate-driven transition of ~27 $(mM\ heme)^{-1}$ (Fig. 7B). Both b_H and b_L transitions had smaller amplitudes in the R74K mutants, at ~14 and ~8 $(mM\ heme)^{-1}$, respectively, for a total of ~22 $(mM\ heme)^{-1}$. The b_{VL} component was too small to be analyzed in the wildtype and in R74K. The R74Q, R74T and R74Y mutants had increasingly smaller b_H and b_L transition amplitudes, decreasing from ~13 and ~8 to ~2 and ~3 $(mM\ heme)^{-1}$, respectively, with no further decrease observed in R74A (Fig. 7B). The amplitude of the b_{VL} transition, observed in R74Q, R74T, R74Y and R74A, did not increase as the b_H and b_L transitions got smaller. As a result, the total amplitude of ascorbate-driven transitions ($b_H + b_L + b_{VL}$) decreased in the R74K => R74A series of mutants.

The heme centers in the purified Arg74 mutants were also characterized by EPR spectroscopy. The low spin heme region of the EPR is shown in Fig. 8; the variation in signal/noise ratio among samples reflects the differences in heme concentration due to different expression efficiencies (Supplementary Material, Table S3). Each of the Arg74 mutants exhibited a distinct signal at g = 3.7, reflecting the presence of the b_L heme center. The proportion of intact b_L center, assessed by the normalized amplitude of the g = 3.7 signal, declined in the order: WT > R74K > R74Q > R74T ~ R74Y ~ R74A (Fig. S7, Supplementary Material). An EPR signal at g = 3.13, reflecting the b_H heme center, was discernable in R74K and R74T, and perhaps in R74Q and R74Y; this signal is clearly absent in R74A (Fig. 8). The EPR signal amplitude near g = 3.13 declined in the order: WT > R74K > R74Q ~ R74T > R74Y > R74A (Figs. 8 and S7). An EPR signal at g = 2.95, ascribed to recombinant cyt b_{561} with b-type heme center in a relaxed conformation (6), was evident in each of the Arg74 mutants but not in the wildtype cytochrome (Fig. 8). The intensity of the g = 2.95 increased in the order: WT < R74K < R74Q ~ R74T < R74Y < R74A (Fig. S7). Finally, EPR signals from multiple species of high spin ferric heme were present near g = 6 in all the samples; with the exception of R74T, the intensity of the g = 6 signals increased monotonically in the R74K => R74A series of mutants (data not shown).

Overall, the pattern of decreases in the native b_H and b_L EPR signals (g = 3.1 and g = 3.7, respectively) for the series of Arg74 mutants (Fig. S7) generally paralleled the pattern of decreasing amplitudes of the b_H and b_L transitions observed in the ascorbate titrations (Fig. 7B). In addition, the trend in the non-native EPR signal at g = 2.95 was opposite that of the native EPR signals (Figs. 8 and S7). This consistent pattern of native vs. non-native components in the titration and EPR analyses indicates that replacing the positively charged sidechain at Arg74 with progressively less conservative substitutions decreased the fraction of recombinant hemoprotein carrying functional b_H and b_L centers.

DISCUSSION

Characterization of ascorbate interactions of cyt b_{561} by spectrophotometric titration

Physiological functioning of cyt b_{561} requires its reduction by cytoplasmic ascorbate (1), and the efficiency of reduction of the two heme centers can be quantitated as the midpoint ascorbate concentrations of the two redox transitions. The C_H and C_L values found here for purified bovine cyt b_{561} wildtype agree well with those reported in earlier studies (Table 1), supporting the reproducibility of the titration approach. Ascorbate titration of murine cyt b_{561} gave a C_H value 45–90% higher than that of the bovine cytochrome (Table 1). As the cyt b_{561}s from the two species have similar b_H redox potentials (3, 11), the difference in C_H values suggests that murine cyt b_{561} has a slightly less efficient interaction with ascorbate. The difference between murine and bovine cytochromes is more dramatic for C_L, being ~4-fold higher in the murine cytochrome, presumably at least partially due to its lower b_H redox potential (19 mV for murine cyt b_{561} vs. 60 mV for bovine cyt b_{561} (3, 11)). Ascorbate titration has also been used to characterize the human and murine forms of duodenal cyt b_{561} (Dcytb), another member of the cyt b_{561} family (26); examination of the C_H and C_L values (Table 1) indicate that the ascorbate reduction efficiencies of the heme centers in these cytochromes are comparable to those of murine adrenal cyt b_{561}. The pattern of distinct ascorbate reduction efficiencies of the two heme centers also has been observed in the tonoplast cyt b_{561} from Arabidopsis (Table 1) (27), suggesting that it may be a general property of the cyt b_{561} family. Interestingly, an alanine mutant of the tonoplast cytochrome in the residue corresponding to Lys85 in adrenal cyt b_{561} markedly impaired reduction by ascorbate (27). This was ascribed to a large increase in the value of C_L, but the generation of ascorbate resistant or refractory species similar to b_{VL} and b_X encountered in the Arg74 mutants (Figs. 7–9) should also be considered.

It is tempting to consider the C_H and C_L values from ascorbate titrations as affinity constants for ascorbate binding, but this is almost certainly mistaken. For one thing, the interaction of ascorbate with the b_H and b_L centers involves both a redox step and a binding step. In addition, ascorbate is converted to semidehydroascorbate, which undergoes several further reactions, some irreversible (28), thereby making true equilibration impossible. The fact that the C_H values were generally comparable to the concentration of cyt b_{561} used for titration raises the possibility that the C_H value might be sensitive to the cytochrome level used. However, replicate titrations of several wildtype and mutant samples at cytochrome concentrations of 6 – 14 μM gave no indication of a systematic variation in C_H with cytochrome level (data not shown). The accumulated experience with ascorbate titrations of cyt b_{561} (Refs. (7, 11, 29) and Figs. 3, 5, and 7) indicates that C_H and C_L values are useful and reproducible as empirical indicators of the efficiency of b_H and b_L reduction by ascorbate. It is worth noting that ascorbate titrations, which combine effects on ascorbate binding and on subsequent redox steps, can be more informative than potentiometric titrations with a non-selective reductant (dithionite) that reflect only the redox properties of the heme centers. For example, the midpoint potentials of the H92Q mutant were indistinguishable from the wildtype values, whereas the C_H value was markedly elevated in the mutant (7). Further, the Arg74 mutant results (Figs. 7 and 8) show that ascorbate titration can assess the proportions of native and non-native protein species and thus evaluate the roles of individual residues in formation of native cytochrome.

EM3 structure and ascorbate titration parameters

The b_H and b_L spectra are known to be sensitive to structural changes in the heme centers (7). Thus, the lack of major effect on the b_H and b_L spectra with all but two of the EM3 alanine mutations indicates that the EM3 structure is largely decoupled from the heme centers' structure. Further, with the exception of R74A, none of the EM3 alanine mutants resulted in substantial amounts of dysfunctional protein (Supplementary Material, Table S2), arguing against longer-range protein structural disruptions. This gives some reassurance that the observed alterations in ascorbate titration parameters in the EM3 mutants can reasonably be attributed to local structural changes.

Many of the alanine mutants in EM3 had alterations in the C_H or C_L (Fig. 5), supporting the earlier general hypothesis that some EM3 residues make important contributions to the redox interactions of cyt b_{561} with ascorbate (4, 10). It is important to note that none of the EM3 alanine mutants completely blocks reduction of the b_H center (Fig. 5). This result implies that no individual EM3 residue is absolutely required for reduction of the b_H heme by ascorbate. This outcome is surprising given the longstanding expectation that one or more conserved EM3 residues would prove crucial to interaction with ascorbate (10). The role of the EM3 segment thus appears more subtle and complex than previously thought. An alanine mutation in Arg72 of murine cyt b_{561} (corresponds to Arg74 in the bovine cytochrome) was reported to lack the b_H transition but retain the b_L transition (11, 29), suggesting selective blockage of ascorbate reduction of b_H. However, the murine R72A titration was incomplete even at ~100 mM ascorbate, indicating the presence of considerable b_{VL} and/or b_X, just as we find with the bovine R74A mutant (Fig. 3). Thus, it remains to be seen whether murine Arg72 mutants actually have coordinated loss of both b_H and b_L.

Several of the mutants gave large increases in the C_H value, namely L70A, L71A, Y73A, R74A, N78A, and K85A (Fig. 5). The effects of the latter four mutants might be ascribed to the loss of electrostatic or polar interactions with the negatively charged and very polar ascorbate. Such charge/polar interactions with substrate are specific to particular positions in EM3, because alanine substitutions at Glu79, Lys81, Arg82, Thr83 or Thr84 had little effect on the C_H value (Fig. 5). Leu70 and Leu71 are predicted to be on the outer face of the TM2 helix (Fig. 6A), so the increases in C_H seen with alanine substitutions at these positions may

reflect disrupted interactions of TM2 with TM1 or TM6 (not included in the model). In this connection, C_H was unchanged in the V72A mutant (Fig. 5), and the Val72 sidechain is predicted to be oriented toward the inside of the four-helix bundle (25). Only one substitution, F76A, resulted in a decrease of C_H past the threshold. Phe76 lies above the b_H heme in the structural model (Fig. 6A), and insertion of the much smaller alanine sidechain at that position might increase access of ascorbate to the heme.

EM3 structure and the b_H and b_L heme centers

None of the alanine mutants in EM3 prevented incorporation of close to the full complement of two hemes (Supplementary Material, Table S2) and most of the mutations had very modest effects on the absorbance spectra of the b_H and b_L heme centers (Fig. 4). Thus, none of the EM3 residues appears to be essential to the "kernel", the structural core of cyt b_{561} whose modification (e.g., by mutation of any one axial heme ligand) results in major structural disruption at both heme centers (6, 7). Two EM3 alanine mutations, Y73A and K85A, did markedly narrow the b_H spectrum (Fig. 4). The distinctive and remarkably similar absence of the shoulder at 554 nm in these two mutants located near opposite ends of EM3 suggested they are structurally linked to each other and to the b_H heme center, a concept supported by the proximity of Tyr73 and Lys85 predicted by the model of Bashtovyy et al. (25) (Fig. 6). The proposed interaction between Lys85 and Tyr73 may be of the 'cation-pi'-type, observed in several transmembrane proteins (30).

EM3 position in relation to the b_H and b_L heme centers

There has been considerable controversy over the disposition of the b_H and b_L centers in adrenal cyt b_{561} with respect to the cytoplasmic and lumenal sides of the chromaffin granule membrane (6, 7, 31). As noted in Results, the effects of EM3 mutations are associated more with b_H than with b_L, indicating that EM3 is physically closer to b_H. Such proximity of EM3 to b_H is consistent with the recent conclusion that the b_H heme ligands are His88 and His161, while the b_L heme ligands are His54 and His122 (6, 7). An earlier topological model for cyt b_{561} puts b_L on the cytoplasmic side, near EM3, based largely on chemical modification studies with DEPC and 4,4′-dithiopyridine (8, 9) and on the presumption that the center with the more negative redox potential (b_L) is exposed to the more reducing compartment, the cytosol (32, 33). Results from chemical modification by DEPC are difficult to interpret conclusively because the reagent produced varying degrees of derivatization of many residues (3, 12). Reaction with dithiopyridine (targeting Cys57 and Cys125 near the heme ligated by His54 and His122, on the matrix side) did decrease the b_H EPR signal (g = 3.1), but the lack of a significant b_L EPR signal (g = 3.7) in the same sample (9) left open the possibility that the sulfhydryl reagent actually perturbed both heme centers. In this connection, disruption of both heme centers is seen with even relatively conservative point mutations at His54 or His122 (6). As for the presumption that the electron from cytoplasmic ascorbate enters cyt b_{561} at b_L, flows to b_H and exits to an acceptor on the matrix side (31), electron flow in the opposite direction, from b_H to b_L, can be demonstrated in the diheme cytochromes of bacterial and mammalian bc1 complexes and bacterial quinol fumarate reductase (34–36). Thus, the accumulating evidence indicates that adrenal cyt b_{561} does indeed have its b_H heme center near the cytoplasmic face of the membrane, and any cyt b_{561} mechanism needs to account for the consequent thermodynamically "uphill" electron transfer. While this manuscript was in review, Desmet et al. reported a cytoplasmic topology for the high-potential heme of a cyt b_{561} analog in Arabidopsis tonoplasts (37). With two examples of cytoplasmic orientation of b_H now in hand, it remains to be seen how general this topology is among other members of the cyt b_{561} family.

Arg74 and structural integrity of the b_H/b_L unit

R74A was the only alanine mutant that exhibited a major decrease in ascorbate reducibility of the cytochrome (Supplementary Material, Table S2). Alteration of sidechain structure at position 74 affected both heme centers, with b_H and b_L content decreasing in concert as progressively more radical substitutions were made (Figs. 7, 8 and S7, and Table S2). Coordinated effects on both heme centers in adrenal cyt b_{561} are a hallmark of single mutations in any one of the four axial heme ligands (6, 7). These similar, pleiotropic effects from mutations in sites that are widely separated in the polypeptide sequence prompted our proposal that the four-helix bundle crosslinked by bis-histidine ligation of the two hemes is part of a larger structural unit or kernel (6, 7). (A recent report (37) indicates that the kernel may be less rigid in a plant tonoplast b_{561} analog.) The coordinated effects of Arg74 on b_H and b_L indicate that the sidechain structure at residue 74 impacts the functional integrity of the kernel. Unlike mutants of the heme axial ligands, even R74A retains two hemes, implying that modifications at Arg74 lead to a more subtle modification of the kernel than does loss of a heme crosslink.

The observed link between the nature of the substitution at Arg74 and extent of loss of the kernel indicated by coordinated decreases in b_H and b_L signal intensities (Figs. 7, 8 and S7) indicates that a positively charged sidechain at residue 74 is critical to formation of the native kernel structure. One possibility is that EM3 forms a key electrostatic interaction via Arg74 to an anionic residue elsewhere on the cytoplasmic side of the cytochrome. An alternative explanation is that the Arg74 sidechain has a charge interaction with a propionate group on the b_H heme. However, disruption of heme propionate-arginine interactions can perturb visible absorption bands (38), and the b_H spectrum is only modestly affected in the Arg74 mutants of cyt b561 (Fig. S4). Further study will be needed to clarify the exact role(s) of Arg74.

As depicted in the scheme in Fig. S8 (Supplementary Material), some of the "lost" b_H/b_L in the Arg74 mutants can be accounted for by protein with weakly functional b_{VL} centers (Fig. 7B), but the majority of the "lost" b_H/b_L appears to reflect recombinant protein carrying heme that is completely refractory to ascorbate (b_X). This ascorbate-refractory fraction is not simply grossly misfolded protein because the ascorbate-refractory species is extractable by mild detergent, and it retains b-type heme that is reducible by dithionite. Rather, it appears that either the ascorbate binding site is lost in the ascorbate-refractory fraction or the redox potential of its heme is shifted significantly below that of ascorbate.

EM3 residue functions in other cytochrome b_{561} family members

Seven of the fifteen residues in the segment of bovine cyt b_{561} examined by alanine scanning are well conserved among the homologous proteins (Fig. 9). Arg74, where mutation to remove the positive charge disrupted formation of the kernel (Figs. 7, 8 and S8) is completely conserved, suggesting that Arg74 is an important shared structural determinant. Tyr73 and Lys85, whose alanine mutants exhibited similar narrowing in b_H spectrum (Fig. 4), are both conserved in all but one of the homologs, suggesting that the proposed interaction between Tyr73 and Lys85 (Fig. 6) is another shared structural feature. Among the positions where alanine mutants had increases in C_H value (Fig. 5), all but Leu70 and Asn78 are well conserved; Phe76, where alanine mutation decreased C_H, is also strongly conserved. Only one mutant in a strongly conserved residue, K81A, did not show a perturbed C_H value (Fig. 5). This general conservation of residues linked by the alanine scanning results to reduction of b_H suggests that the cyt b_{561} homologs share a common mechanism for ascorbate interaction on the cytoplasmic face of the cytochrome.

In summary, the cytoplasmic EM3 segment of adrenal cyt b_{561} has often been implicated in the interaction of with ascorbate. The present alanine scanning study provides the first systematic evaluation of the roles of individual residues in this segment. The results identify several EM3 residues linked to the efficiency of cyt b_{561} reduction by ascorbate, two residues that influence the alpha band spectrum of the b_H heme center, and one residue that is important to the integrity of the structural unit carrying both heme centers. These findings substantially increase understanding of the structural and functional relationships between EM3 residues and the heme centers in this important cytochrome.

Supplementary Material

Refer to Web version on PubMed Central for supplementary material.

Acknowledgments

We thank Dr. Yury Kamensky (Rice University) for helpful discussions and Dr. Han Asard (University of Antwerp) for sharing the coordinates for the cyt b_{561} structural model.

References

1. Njus D, Kelley PM. The secretory-vesicle ascorbate-regenerating system: a chain of concerted H+/e(−)-transfer reactions. Biochim Biophys Acta. 1993; 1144:235–248. [PubMed: 8399278]
2. Apps DK, Boisclair MD, Gavine FS, Pettigrew GW. Unusual redox behaviour of cytochrome b-561 from bovine chromaffin granule membranes. Biochim Biophys Acta. 1984; 764:8–16. [PubMed: 6696883]
3. Takeuchi F, Kobayashi K, Tagawa S, Tsubaki M. Ascorbate inhibits the carbethoxylation of two histidyl and one tyrosyl residues indispensable for the transmembrane electron transfer reaction of cytochrome b561. Biochemistry. 2001; 40:4067–4076. [PubMed: 11300787]
4. Tsubaki M, Takeuchi F, Nakanishi N. Cytochrome b561 protein family: expanding roles and versatile transmembrane electron transfer abilities as predicted by a new classification system and protein sequence motif analyses. Biochim Biophys Acta. 2005; 1753:174–190. [PubMed: 16169296]
5. Perin MS, Fried VA, Slaughter CA, Sudhof TC. The structure of cytochrome b561, a secretory vesicle-specific electron transport protein. Embo J. 1988; 7:2697–2703. [PubMed: 2460342]
6. Kamensky Y, Liu W, Tsai AL, Kulmacz RJ, Palmer G. Axial ligation and stoichiometry of heme centers in adrenal cytochrome b561. Biochemistry. 2007; 46:8647–8658. [PubMed: 17602662]
7. Liu W, Rogge CE, da Silva GF, Shinkarev VP, Tsai AL, Kamensky Y, Palmer G, Kulmacz RJ. His92 and His110 selectively affect different heme centers of adrenal cytochrome b561. Biochim Biophys Acta. 2008; 1777:1218–1228. [PubMed: 18501187]
8. Takeuchi F, Hori H, Obayashi E, Shiro Y, Tsubaki M. Properties of two distinct heme centers of cytochrome b561 from bovine chromaffin vesicles studied by EPR, resonance Raman, and ascorbate reduction assay. J Biochem (Tokyo). 2004; 135:53–64. [PubMed: 14999009]
9. Takeuchi F, Hori H, Tsubaki M. Selective Perturbation of the Intravesicular Heme Center of Cytochrome b561 by Cysteinyl Modification with 4,4′-Dithiodipyridine. J Biochem (Tokyo). 2005; 138:751–762. [PubMed: 16428304]
10. Okuyama E, Yamamoto R, Ichikawa Y, Tsubaki M. Structural basis for the electron transfer across the chromaffin vesicle membranes catalyzed by cytochrome b561: analyses of cDNA nucleotide sequences and visible absorption spectra. Biochim Biophys Acta. 1998; 1383:269–278. [PubMed: 9602148]
11. Berczi A, Su D, Lakshminarasimhan M, Vargas A, Asard H. Heterologous expression and site-directed mutagenesis of an ascorbate-reducible cytochrome b561. Arch Biochem Biophys. 2005; 443:82–92. [PubMed: 16256064]
12. Tsubaki M, Kobayashi K, Ichise T, Takeuchi F, Tagawa S. Diethyl pyrocarbonate modification abolishes fast electron accepting ability of cytochrome b561 from ascorbate but does not influence

electron donation to monodehydroascorbate radical: identification of the modification sites by mass spectrometric analysis. Biochemistry. 2000; 39:3276–3284. [PubMed: 10727219]

13. Kipp BH, Kelley PM, Njus D. Evidence for an essential histidine residue in the ascorbate-binding site of cytochrome b561. Biochemistry. 2001; 40:3931–3937. [PubMed: 11300772]
14. Takigami T, Takeuchi F, Nakagawa M, Hase T, Tsubaki M. Stopped-flow analyses on the reaction of ascorbate with cytochrome b561 purified from bovine chromaffin vesicle membranes. Biochemistry. 2003; 42:8110–8118. [PubMed: 12846560]
15. Hulme EC, Bee MS, Goodwin JA. Phenotypic classification of mutants: a tool for understanding ligand binding and activation of muscarinic acetylcholine receptors. Biochem Soc Trans. 2007; 35:742–745. [PubMed: 17635138]
16. Liu W, Rogge CE, Kamensky Y, Tsai AL, Kulmacz RJ. Development of a bacterial system for high yield expression of fully functional adrenal cytochrome b561. Protein Expr Purif. 2007; 56:145–152. [PubMed: 17521920]
17. Peterson GL. A simplification of the protein assay method of Lowry *et al*. which is more generally applicable. Analytical Biochemistry. 1977; 83:346–356. [PubMed: 603028]
18. Liu W, Kamensky Y, Kakkar R, Foley E, Kulmacz RJ, Palmer G. Purification and characterization of bovine adrenal cytochrome b561 expressed in insect and yeast cell systems. Protein Expr Purif. 2005; 40:429–439. [PubMed: 15766887]
19. Berry EA, Trumpower BL. Simultaneous determination of hemes a, b, and c from pyridine hemochrome spectra. Anal Biochem. 1987; 161:1–15. [PubMed: 3578775]
20. Kulmacz RJ, Tsai AL, Palmer G. Heme spin states and peroxide-induced radical species in prostaglandin H synthase. J Biol Chem. 1987; 262:10524–10531. [PubMed: 3038886]
21. Laemmli UK. Cleavage of structural proteins during the assembly of the head of bacteriophage T4. Nature. 1970; 227:680–685. [PubMed: 5432063]
22. Berczi A, Desmet F, Van Doorslaer S, Asard H. Spectral characterization of the recombinant mouse tumor suppressor 101F6 protein. Eur Biophys J. 2010; 39:1129–1142. [PubMed: 19943161]
23. Barker PD, Ferrer JC, Mylrajan M, Loehr TM, Feng R, Konishi Y, Funk WD, MacGillivray RT, Mauk AG. Transmutation of a heme protein. Proc Natl Acad Sci U S A. 1993; 90:6542–6546. [PubMed: 8341666]
24. Nakanishi N, Takeuchi F, Tsubaki M. Histidine cycle mechanism for the concerted proton/electron transfer from ascorbate to the cytosolic haem b centre of cytochrome b561: a unique machinery for the biological transmembrane electron transfer. J Biochem. 2007; 142:553–560. [PubMed: 17905810]
25. Bashtovyy D, Berczi A, Asard H, Pali T. Structure prediction for the di-heme cytochrome b561 protein family. Protoplasma. 2003; 221:31–40. [PubMed: 12768339]
26. Su D, May JM, Koury MJ, Asard H. Human erythrocyte membranes contain a cytochrome b561 that may be involved in extracellular ascorbate recycling. J Biol Chem. 2006; 281:39852–39859. [PubMed: 17068337]
27. Berczi A, Asard H. Characterization of an ascorbate-reducible cytochrome b561 by site-directed mutagenesis. Acta Biol Szeged. 2006; 50:55–59.
28. Linster CL, Van Schaftingen E. Vitamin C. Biosynthesis, recycling and degradation in mammals. FEBS J. 2007; 274:1–22. [PubMed: 17222174]
29. Lakshminarasimhan M, Berczi A, Asard H. Substrate-dependent reduction of a recombinant chromaffin granule Cyt-b561 and its R72A mutant. Acta Biol Szeged. 2006; 50:61–65.
30. Gromiha MM. Influence of cation-pi interactions in different folding types of membrane proteins. Biophys Chem. 2003; 103:251–258. [PubMed: 12727287]
31. Nakanishi N, Rahman MM, Sakamoto Y, Takigami T, Kobayashi K, Hori H, Hase T, Park SY, Tsubaki M. Importance of the conserved lysine 83 residue of Zea mays cytochrome b(561) for ascorbate-specific transmembrane electron transfer as revealed by site-directed mutagenesis studies. Biochemistry. 2009; 48:10665–10678. [PubMed: 19803484]
32. Tsubaki M, Nakayama M, Okuyama E, Ichikawa Y, Hori H. Existence of two heme B centers in cytochrome b561 from bovine adrenal chromaffin vesicles as revealed by a new purification procedure and EPR spectroscopy. J Biol Chem. 1997; 272:23206–23210. [PubMed: 9287327]

33. Kobayashi K, Tsubaki M, Tagawa S. Distinct roles of two heme centers for transmembrane electron transfer in cytochrome b561 from bovine adrenal chromaffin vesicles as revealed by pulse radiolysis. J Biol Chem. 1998; 273:16038–16042. [PubMed: 9632654]

34. Osyczka A, Moser CC, Daldal F, Dutton PL. Reversible redox energy coupling in electron transfer chains. Nature. 2004; 427:607–612. [PubMed: 14961113]

35. Miki T, Umeda M, Harada Y. Inhibition of reversed electron transfer and proton transport in the beef heart cytochrome bc1 complex by chemical modification. J Biochem. 2007; 141:377–387. [PubMed: 17234684]

36. Haas AH, Lancaster CR. Calculated coupling of transmembrane electron and proton transfer in dihemic quinol:fumarate reductase. Biophys J. 2004; 87:4298–4315. [PubMed: 15361415]

37. Desmet F, Berczi A, Zimanyi L, Asard H, Van Doorslaer S. Axial ligation of the high-potential heme center in an Arabidopsis cytochrome b561. FEBS Lett. 2011; 585:545–548. [PubMed: 21236254]

38. Lee HJ, Ojemyr L, Vakkasoglu A, Brzezinski P, Gennis RB. Properties of Arg481 mutants of the aa3-type cytochrome c oxidase from Rhodobacter sphaeroides suggest that neither R481 nor the nearby D-propionate of heme a3 is likely to be the proton loading site of the proton pump. Biochemistry. 2009; 48:7123–7131. [PubMed: 19575527]

39. Viklund H, Elofsson A. OCTOPUS: improving topology prediction by two-track ANN-based preference scores and an extended topological grammar. Bioinformatics. 2008; 24:1662–1668. [PubMed: 18474507]

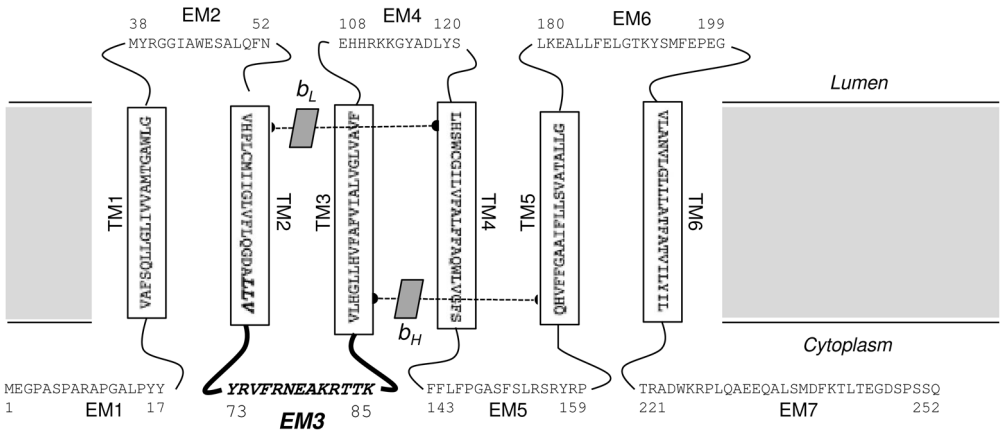

Fig 1.

Model for the membrane topology of adrenal cyt b_{561} showing the predicted (39) transmembrane segments (TM1–TM6) and extramembrane segments (EM1–EM7). The orientation of b_H and b_L heme centers is based on earlier mutagenic studies (6, 7).

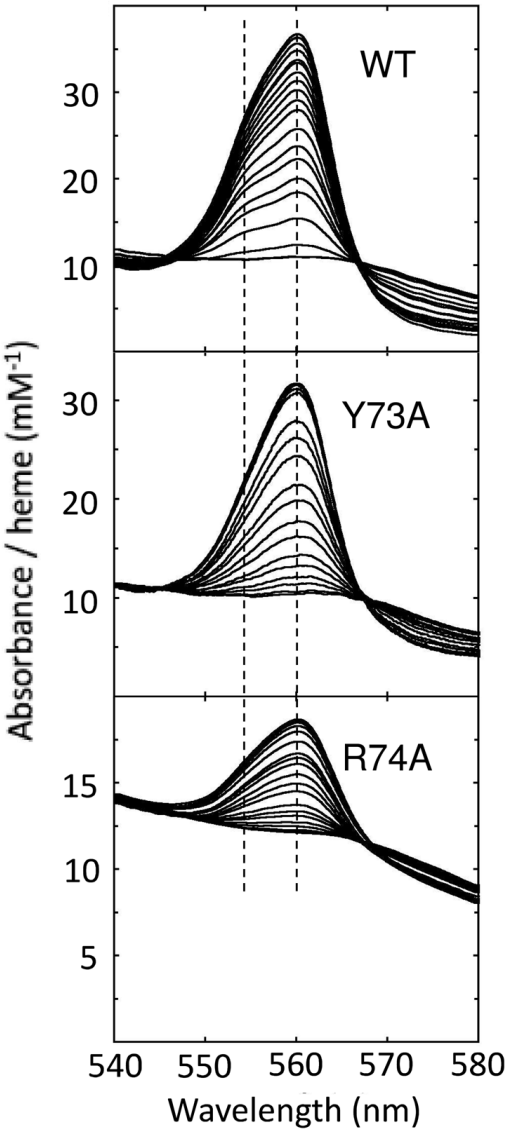

Fig 2.

Increases in alpha-band absorbance during ascorbate titrations of wildtype (0–30 mM Asc) (top), Y73A (0–20 mM Asc) (middle) and R74A (0–90 mM Asc) (bottom).

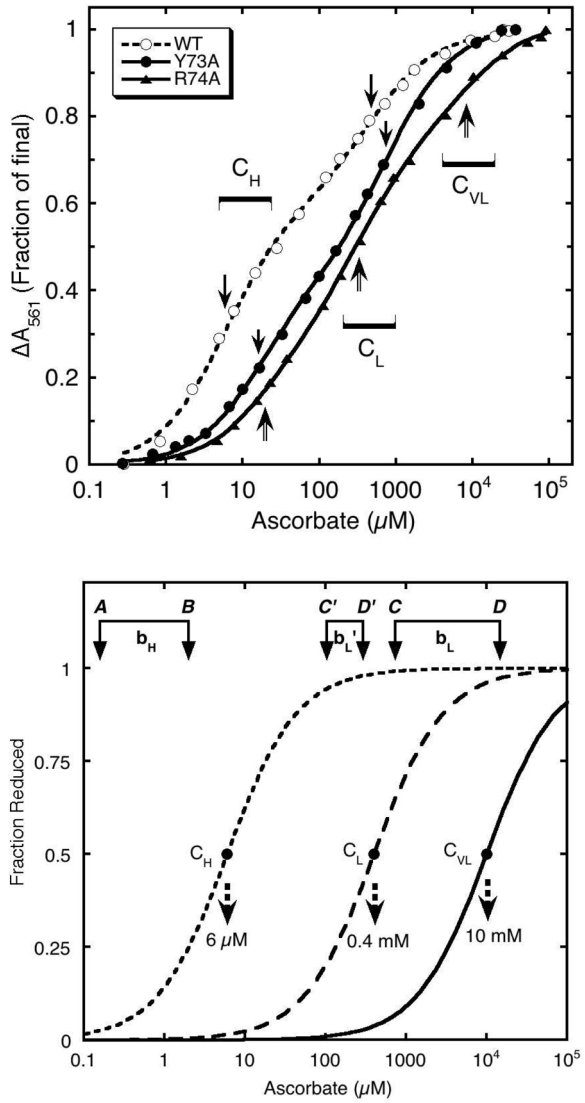

Fig. 3.

Ascorbate titration curves. Top: Titrations of wildtype (WT) cyt b_{561} and the Y73A and R74A mutants. ΔA values are normalized to the Δ A at the highest ascorbate concentration. Bottom: Predicted reductive transitions (Eq. 2) for heme centers with midpoint ascorbate concentrations typical for b_H, b_L and b_{VL}. Brackets indicate the titration stages where difference spectra were obtained for b_H (spectrum B – spectrum A), b_L (spectrum D – spectrum C), and b_L in the presence of b_{VL} ($b_{L'}$, spectrum D′ – spectrum C′).

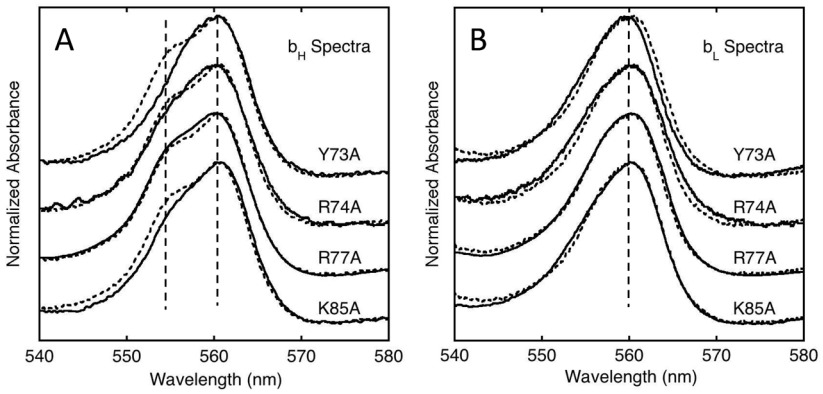

Fig 4.

Difference spectra for b_H (A) and b_L (B) in selected EM3 alanine mutants determined from ascorbate titration data as indicated in Fig. 3. The spectra shown are averages of difference spectra from two separate titrations, with each mutant spectrum (solid line) superimposed on wildtype spectrum (dashed line).

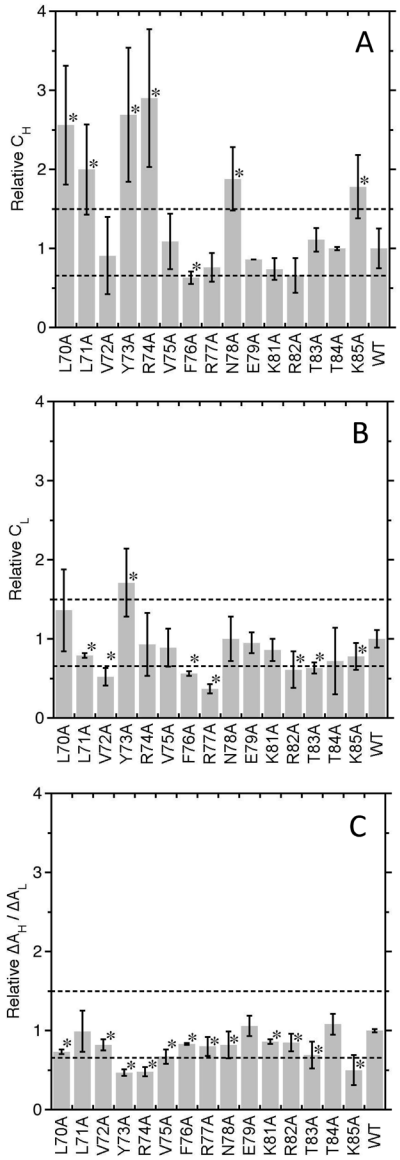

Fig. 5.

Ascorbate titration parameters for EM3 alanine mutants, Average values for C_H (A), C_L (B) and $\Delta A_H/\Delta A_L$ (C) were normalized to the corresponding wildtype (WT) values (C_H, 5.3 μM; C_L, 394 μM; $\Delta A_H/\Delta A_L$, 1.50). Error bars indicate SD for n = 2–6 titrations (n=7 for WT). Asterisks indicate a statistically significant difference from the WT value ($p < 0.05$). Horizontal dashed lines represent an increase or attenuation by a factor of 1.5.

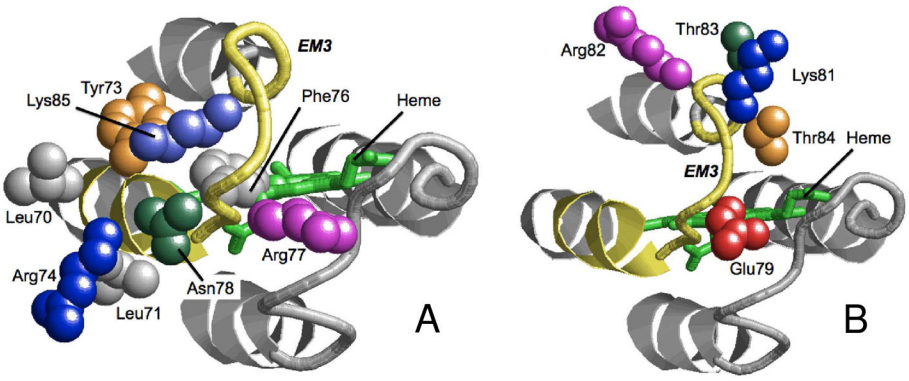

Fig. 6.

Computational structural model of the b_H heme region of cyt b_{561} (25) showing the positions of targeted residues in EM3 and flanking residues (backbone shown in yellow). Panel A highlights residues where mutation significantly altered one or more ascorbate titration parameters; Panel B highlights residues where mutation had little or no impact.

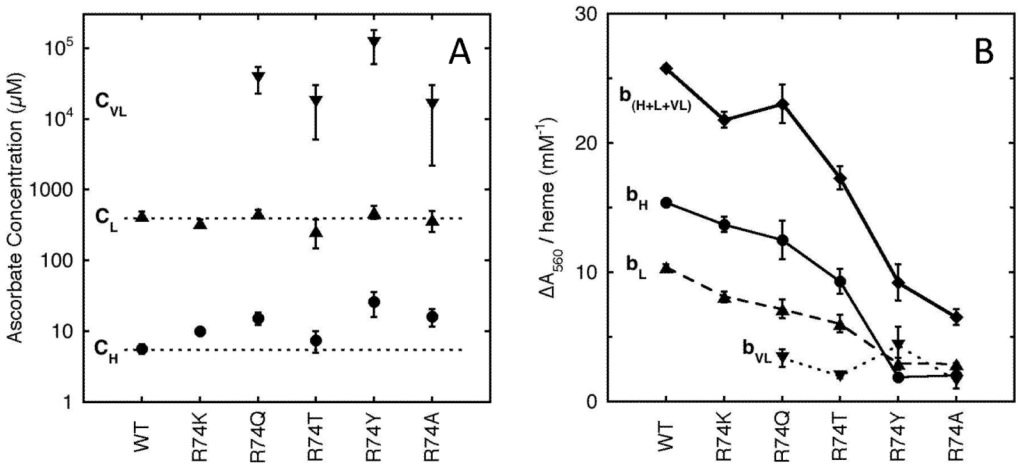

Fig 7.

Ascorbate titration parameters for wildtype (WT) cyt b561 and the Arg74 mutants. Panel A: Midpoint ascorbate concentrations for the high-potential (C_H), low-potential (C_L) and very low-potential (C_{VL}), types of heme center transition. Panel B: Absorbance change amplitudes for the individual transitions and their sum. The third transition at high ascorbate levels was negligible for wildtype and the R74K mutant.

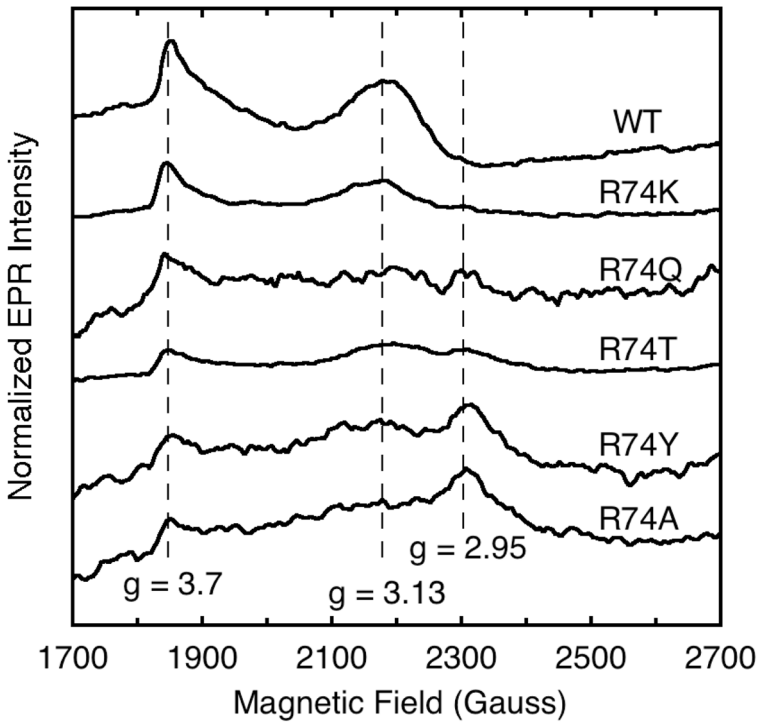

Fig. 8.

Low spin heme region of the EPR spectra of wildtype (WT) cyt b561 and the Arg74 mutants in the ferric state. Amplitudes are normalized to total heme concentration (in μM): WT, 143 μM; R74K, 150; R74Q, 32; R74T, 102; R74Y, 45; and R74A, 50. The temperature was 4 K except for WT (8 K).

```
                                          70    75    80    85
                                          |     |     |     |
                  conserved >85% => G***L*YR*FR***K***K*LH
                     kernel defect =>     ****R*****  *****
                  altered bH spectrum =>  ***Y******  ****K
                     altered CH value =>  LL*YR*F*N*  ****K

IDENTIFIER     ORGANISM
P10897         B. taurus              67 GDALLVYRVFRNEAKRTTKVLH
NP001125175    P. abelii              66 GDALLVYRVFRNEAKRTTKVLH
XP001495680    E. caballus            62 GDALLVYRVFRNEAKRTTKVLH
EFB24487       A. melanoleuca         60 GDALLVYRVFRNEAKRTTKVLH
XP853258       C. familiaris          67 GDALLVYRVFRNEAKRTTKVLH
NP001087259    O. aries               67 GDALLVYRVFRNEAKRTTKVLH
NP001906       H. sapiens             66 GNALLVYRVFRNEAKRTTKVLH
NP001090991    S. scrofa              67 GDALLVYRVFRNEAKRTTKILH
NP001100526    R. norvegicus          65 GDALLVYRVFRKEAKRTTKILH
AAA65643       M. musculus            65 GDALLVYRVFRREAKRTTKILH
NP001089047    X. laevis              66 GEALLVYRVFRHETKRSTKILH
NP001005633    X. tropicalis          65 GEALLVYRVFRHETKRATKILH
NP001122216    D. rerio               61 GDAVLVYRVFRNESKRSVKILH
CAG05955       T. nigroviridis        53 GDAIVVYRVFHNESKRTIKMLH
NP499095       C. elegans             76 GEALLVYRVFRNERKKFSKTLH
XP002641730    C. briggsae            76 GESILVYRVFRNERKKFSKTLH
XP001894183    B. malayi              71 GDGILVYRIFRHERKRFSKLLH
XP002574073    S. mansoni             71 GDAILVYRVFRSFRKLPIKILH
XP001635650    N. vectensis           69 SEAMIVYRVFRNETKYTVKLVH
ACO10642       C. rogercresseyi       66 GNGMLVYRNFRGEAKKRLKILH
ACO15392       C. clemensi            66 GNGMLVYRNFRGEAKKRLKLLH
ACI90364       P. roseola             73 GDAILAYRVFRDVKKIRVKILH
BAB32556       D. japonica            76 GNAIMVYRVFRNTKKIRAKWLH
XP002635501    C. briggsae            85 GEALLAYRVYRHDAKMVSKLLH
XP002595114    B. floridae            83 GNAILTYRVFRDQVKLGVKILH
NP001041449    C. intestinalis        70 GEAALVYRVFRQTEKLKAKIIH
XP002160113    H. magnipapillata      81 GNAAIAYRVFRNQNKLKIKILH
CAX70071       S. japonicum           71 GDSILVFRVFRSYRKLPVKILH
NP001023900    C. elegans             80 GEALLAYRLYRYDAKIISKLLH
XP002426701    P. humanus             64 ANGILVYRSFRNSRKRKLKIAH
XP001656283    A. aegypti             69 GNSILVYRGFRYARKKPLKVTH
```

Fig. 9.

Alignment of EM3 segments and flanking residues in bovine adrenal cyt b_{561} homologs from several organisms. The numbering of the bovine cyt b_{561} residues under study is shown at top, along with conserved residues and residues where alanine substitution affected the kernel structure, the b_H spectrum or the C_H value.

Table 1

Comparison of ascorbate titration parameters for wildtype cyt b_{561} and for Dcytb.

Protein	C_H (μM)	C_L (μM)	Reference
Bovine cyt b_{561} (endogenous) purified	11 ± 1	360 ± 50	(11)
Bovine cyt b_{561} (recombinant) purified	5.4 ± 1.5	369 ± 119	(7)
Bovine cyt b_{561} (recombinant) purified	5.3 ± 2.0	394 ± 79	present study
Murine cyt b_{561} (yeast) membranous	16 ± 5	1240 ± 190	(11)
Murine cyt b_{561} (yeast) purified	21 ± 6	1500 ± 500	(29)
Murine Dcytb (yeast) membranous	70 ± 20	1820 ± 140	(26)
Human Dcytb (endogenous) membranous	10 ± 0	770 ± 230	(26)
Arabidopsis cyt b_{561} (yeast) membranous	<100 (?)	~1500	(27)